CLASSICAL NETWORK THEORY ASPECT OF NO-PASS FILTERS

by

TEJINDER SINGH RAJPAL

B. A., Panjab University, Chandigarh, India, 1958
B. Sc. Engg., Thapar Engineering College, 1962
Patiala, Panjab, India

A MASTER'S REPORT

submitted in partial fulfillment of the

requirements for the degree

MASTER OF SCIENCE

Department of Electrical Engineering

KANSAS STATE UNIVERSITY
Manhattan, Kansas

1964

Approved by:

Charles A. Halijak

Major Professor

TABLE OF CONTENTS

INTRODUCTION

A filter is a network designed to pass certain bands of frequencies with low attenuation and cause very high attenuation to unwanted frequencies. In classical network theory, filters are classified in accordance with their frequency characteristics as follows: low-pass filters, high-pass filters, band-pass filters, band-elimination filters and all-pass filters. When a low-pass filter and a high-pass filter are cascaded, the result is a band-pass filter, provided cut-off frequency of the low-pass filter ω_c' is greater than that of the high-pass filter ω_c. But in case $\omega_c' \leqslant \omega_c$, the result is a no-pass filter. Since the cascaded network in the above case attenuates highly signals of all frequencies, the combination is called a no-pass filter.

In this report characteristic impedance degradation has been used to physically realize the no-pass filter. The characteristic impedance degradation is achieved by left and right terminating a low-pass filter with high-pass half-end-sections. This method is antithetical to Zobel's half-end-sections method of characteristic impedance improvement but emphasizes mismatching.

The interactance of a filter is defined as the ratio of the power dissipated in the source resistance with the filter in circuit to the power which would be dissipated when a pure resistor equal to the source resistance replaces the filter in the circuit.

ZOBEL'S CHARACTERISTIC IMPEDANCE IMPROVEMENT METHOD

O. J. Zobel (5) removed a shortcoming of constant-K filter design as regards characteristic impedance variation in the pass-band. He improved it by addition of one section of a different type on each end of a filter. These added half-sections are m-derived half sections; and the related constant-K section is called prototype. This characteristic impedance improvement method was based upon the assumption that the filter involved was terminated in characteristic impedance. The characteristic impedance of the composite network (see Fig. 4) consisting of prototype P of Fig. 1 and Zobel's m-derived half-sections N and N' of Fig. 3 is found as follows by the use of Cayley's notation (for Cayley's notation see Appendix).

Given: (see Fig. 4)

$$P(\mathcal{J}) = \mathcal{J} \tag{1}$$

$$M(\mathcal{J}) = \mathcal{J} \tag{2}$$

$$M(\mathcal{J}) = NN'(\mathcal{J}) \tag{3}$$

$$N(K) = \mathcal{J} \tag{4}$$

$$N'(\mathcal{J}) = K \tag{5}$$

where $\mathcal{J}$ is the characteristic impedance of network P in Fig. 1 and k is the characteristic impedance of the composite network in Fig. 4.

The characteristic impedance of the composite network N'PN (see Fig. 4) is found below in equation (6).

$$N'PN(K) = N'P(\mathcal{J}) = N'(\mathcal{J}) = k \tag{6}$$

In case P is a unit low-pass section (see Fig. 5), its

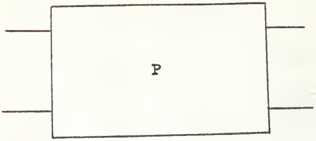

Fig. 1. Prototype P constant-K filter section.

Fig. 2. m-derived section of P in Fig. 1.

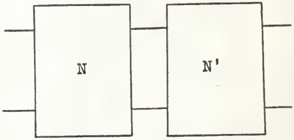

Fig. 3. M in Fig. 2 split into two symmetrical halves.

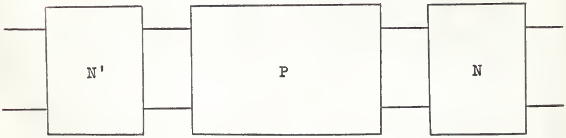

Fig. 4. Composite network, consisting of P in Fig. 1 and its m-derived end-sections in Fig. 3.

m-derived section is found to be as in Fig. 6. The m-derived section is split into two halves as N and N' (see Fig. 7) and the composite network is shown in Fig. 8. The characteristic impedance of the network N'PN (see Fig. 8) is found below.

From equation (6)

$$N'PN(K) = K = N'(\rho)$$

where $\rho = \sqrt{1 + s^2}$

Therefore

$$K = \begin{bmatrix} 1 & 0 \\ \dfrac{ms}{1 + (1-m^2)s^2} & 1 \end{bmatrix} \begin{bmatrix} 1 & ms \\ 0 & 1 \end{bmatrix} (\rho) \qquad (7)$$

$$= \begin{bmatrix} 1 & ms \\ \dfrac{ms}{1 + (1-m^2)s^2} & \dfrac{s^2 + 1}{1 + (1-m^2)s^2} \end{bmatrix} (\rho) \qquad (8)$$

With Cayley's notation, equation (8) can be written as

$$K = \frac{\rho + ms}{\dfrac{ms}{1 + (1-m^2)s^2}\rho + \dfrac{s^2 + 1}{1 + (1-m^2)s^2}} \qquad (9)$$

Substituting the value of ρ, equation (9) yields,

$$K = \left. \frac{1 + (1-m^2)s^2}{\sqrt{1 + s^2}} \right|_{s = j\omega} \qquad (10)$$

The curves of $|K|$ versus angular frequency ω for different values of m in the range $0 < m < 1$, have been plotted in standard network textbooks. It is noted that the characteristic impedance is closest to one when $m = 0.6$ and is nearly constant over a large part of the transmission.

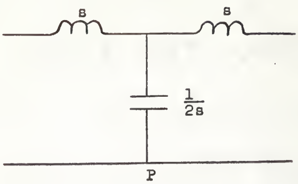

Fig. 5. Unit low-pass section P.

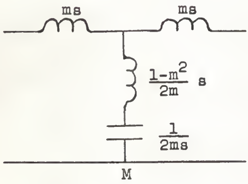

Fig. 6. m-derived of low-pass section in Fig. 5.

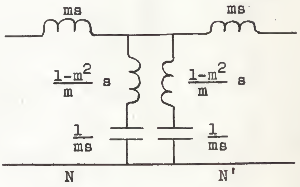

Fig. 7. m-derived section in Fig. 6 split into two symmetric halves.

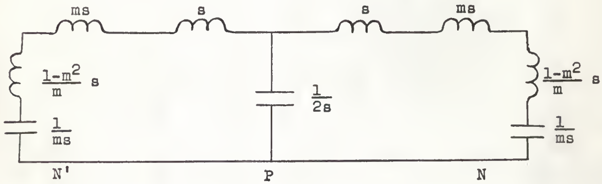

Fig. 8. Composite section consisting of low-pass section in Fig. 5 and its m-derived end sections in Fig. 7.

CHARACTERISTIC IMPEDANCE DEGRADATION

No-pass filters can be realized in the Zobel manner except that m-derivation is replaced by low- to high-pass transformation. The above transformation is accomplished by changing s to 1/s in the low-pass network of Fig. 5. The resulting network's characteristic impedance is reactive in the frequency range of the low-pass network.

The degradation is now demonstrated. From Fig. 5

$$\mathcal{Z}_{Lo} = \sqrt{Z_{msc}\ Z_{moc}} \tag{11}$$

$$= \sqrt{1 + s^2}\,\Big|_{s = j\omega} \tag{12}$$

Evaluating $|\mathcal{Z}_{Lo}|$ by substituting $s = j\omega$ the following result is obtained

$$|\mathcal{Z}_{Lo}| = \sqrt{1 - \omega^2} \tag{13}$$

Similarly from Fig. 9

$$\mathcal{Z}_{Hi} = \sqrt{Z_{msc}\ Z_{moc}} \tag{14}$$

$$= \sqrt{1 + 1/s^2}\,\Big|_{s = j\omega} \tag{15}$$

Evaluating $|\mathcal{Z}_{Hi}|$ by substituting $s = j\omega$ the following result is obtained

$$|\mathcal{Z}_{Hi}| = \sqrt{1 - 1/\omega^2} \tag{16}$$

Figure 10 is drawn from equations (13) and (16), and from that it is observed that

$|\mathcal{Z}_{Lo}|$ is resistive for $0<\omega<1$, $|\mathcal{Z}_{Hi}|$ is reactive for $0<\omega<1$

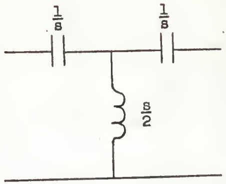

Fig. 9. Network obtained after low- to high-pass transformation on network in Fig. 5.

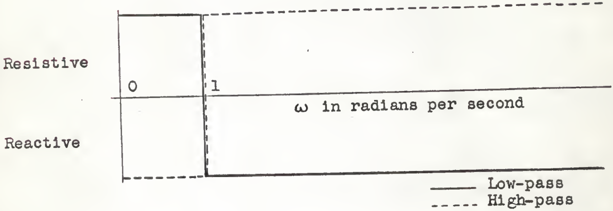

Fig. 10. Behavior of characteristic impedance in case of low- and high-pass networks (see Fig. 5 and Fig. 9 respectively) in all regions.

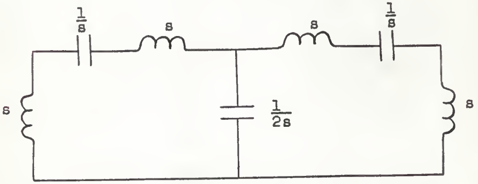

Fig. 11. Composite network consisting of unit low-pass P with half-sections of network in Fig. 9 on ends.

$|\rho_{Lo}|$ is reactive for $1<\omega<\infty$, $|\rho_{Hi}|$ is resistive for $1<\omega<\infty$. So when two half-sections of Fig. 9 are cascaded with low-pass filter prototype of Fig. 5 as shown in Fig. 11, the stated mismatched impedance situation occurs, and characteristic impedance degradation is achieved. But in the network of Fig. 11 the problem of series resonance occurs. In order to avoid short-circuit due to series resonance, another general resistive network (see Fig. 12) having the characteristic impedance ρ_R is introduced. In this case ρ_R is taken as one ohm for simplicity, since ρ_{Lo} is approximately equal to one ohm. Different values can be given to n, the value n = 3 is arbitrarily selected. Since as n is increased further the resistance of the shunt arm goes on decreasing tending to short-circuit condition, while the resistance of the series arm keeps on increasing. So with $\rho_R = 1$ and n = 3, the network of Fig. 12 becomes that in Fig. 13.

The network of Fig. 13 is also split as before and is cascaded with network of Fig. 11, and the resulting network is terminated on both sides with one ohm (see Fig. 14). The network of Fig. 14 attenuates highly signals of both low and high frequencies and is the required no-pass filter.

VOLTAGE TRANSFER FUNCTION OF NO-PASS FILTER

In order to find the voltage transfer function of the no-pass filter (see Fig. 14), the transfer matrix of the above network is found. Since the network in Fig. 14 is symmetric, only the transfer matrix of the left-half of the network (see Fig. 15) need be found and is obtained as follows.

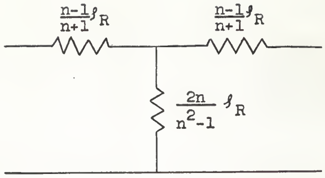

Fig. 12. A general four terminal resistive network having characteristic impedance ρ_R.

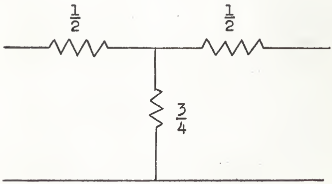

Fig. 13. Network of Fig. 12 when n=3 and ρ_R is taken as 1.

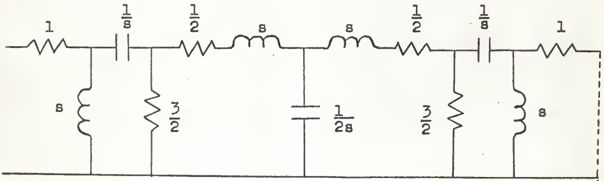

Fig. 14. Network for the realization for the no-pass filter, such that cut-off frequency of both low-pass and high-pass filter is one radian per second.

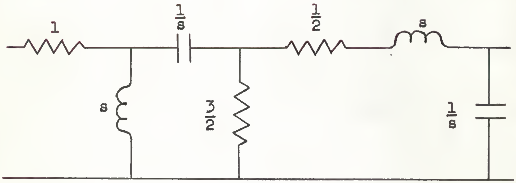

Fig. 15. Left half-section of the symmetric network in Fig. 14.

The half filter's transfer matrix is

$$\begin{bmatrix} \alpha & \beta \\ \gamma & \delta \end{bmatrix} \tag{18}$$

where

$$\alpha = \frac{4 + 18s + 25s^2 + 21s^3 + 10s^4}{6s^2} \tag{19}$$

$$\beta = \frac{8 + 15s + 21s^2 + 10s^3}{6s^2} \tag{20}$$

$$\gamma = \frac{4 + 14s + 11s^2 + 14s^3 + 4s^4}{6s^2} \tag{21}$$

$$\delta = \frac{8 + 7s + 14s^2 + 4s^3}{6s^2} \tag{22}$$

The transfer matrix of the whole filter is

$$\begin{bmatrix} \alpha & \beta \\ \gamma & \delta \end{bmatrix} \begin{bmatrix} \delta & \beta \\ \gamma & \alpha \end{bmatrix}$$

$$= \begin{bmatrix} \alpha\delta + \beta\gamma & 2\alpha\beta \\ 2\gamma\delta & \alpha\delta + \beta\gamma \end{bmatrix} \tag{23}$$

The transfer function of the no-pass filter (see Fig. 14) is

$$\frac{1}{2\alpha\beta} = \left. \frac{0.5s^4}{\begin{array}{c} 0.889 + 5.6667s + 15.389s^2 + 26.694s^3 \\ + 30.556s^4 + 23.361s^5 + 11.667s^6 + 2.777s^7 \end{array}} \right|_{s = j\omega} \tag{24}$$

An IBM 1620 was used to find the data for the spectrum of the above voltage transfer function, when ω varied from 0.01 to 100 radians per second. The spectrum of the voltage transfer function (in decibels) versus ω (in radians per second) is

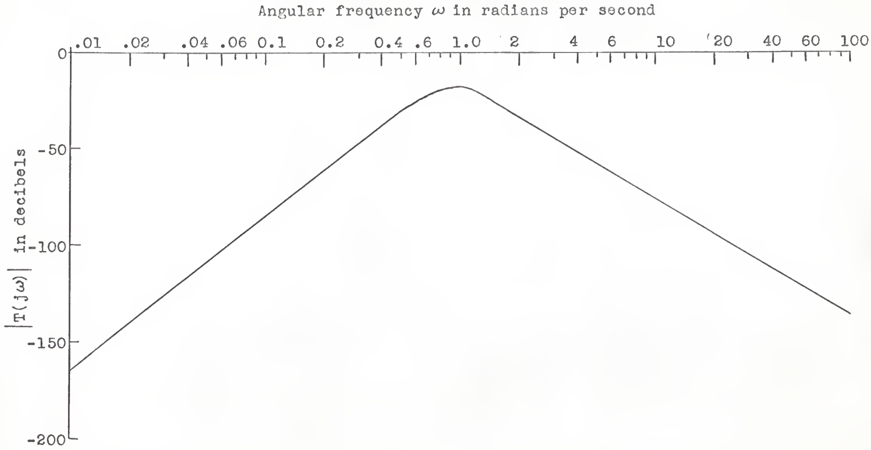

Fig. 16. Frequency response of no-pass filter of Fig. 14.

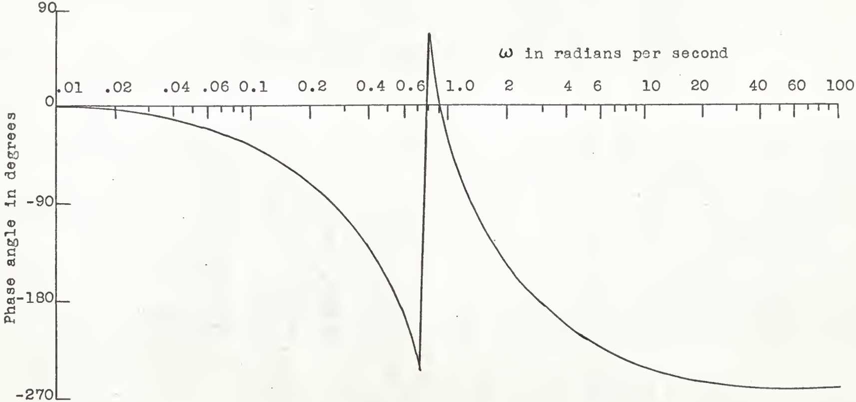

Fig. 17. Phase angle of voltage transfer function of no-pass filter of Fig. 14.

plotted on a semi-log paper (see Fig. 16). The spectrum rises uniformly to a higher value near cut-off frequency (one radian per second) of both low- and high-pass filter, and then again decreases uniformly as the frequency increases. In other words the attenuation on both sides of the cut-off frequency is higher than at the cut-off. The phase angle dependence of this transfer function on frequency is plotted in Fig. 17.

IMPROVEMENT OF NO-PASS FILTER

To improve the response of the voltage transfer function of the no-pass filter in equation (24), the cut-off frequency of the low-pass filter used in Fig. 14 is reduced to $1-\lambda$ radian per second and correspondingly the cut-off frequency of the high-pass in Fig. 14 is raised to $1/(1-\lambda)$ radians per second. $\lambda = 0.5$ is chosen arbitrarily. In order to realize that (see Fig. 14), in low-pass section transformation $s \longrightarrow \frac{s}{1-\lambda} = 2s$, and in high-pass section transformation $s \longrightarrow (1-\lambda)s = s/2$ are done. The resulting network is shown in Fig. 18. The transfer matrix of the new network in Fig. 18 is

$$\begin{bmatrix} A & B \\ C & D \end{bmatrix} \begin{bmatrix} D & B \\ C & A \end{bmatrix}$$

$$= \begin{bmatrix} AD + BC & 2AB \\ 2CD & AD + BC \end{bmatrix} \tag{25}$$

where

$$A = \frac{8 + 42s + 59s^2 + 51s^3 + 20s^4}{3s^2} \tag{26}$$

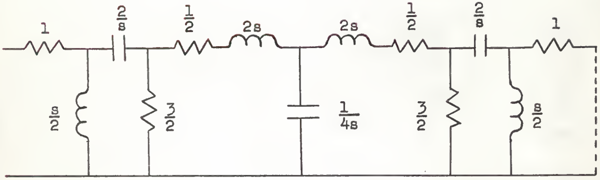

Fig. 18. Network for the realization of improved no-pass filter, such that cut-off frequency of low-pass filter is 1/2 radian per second and cut-off of high-pass filter is 2 radians per second.

$$B = \frac{16 + 27s + 25.5s^2 + 10s^3}{3s^2} \tag{27}$$

$$C = \frac{8 + 38s + 40s^2 + 32s^3 + 8s^4}{3s^2} \tag{28}$$

$$D = \frac{16 + 19s + 16s^2 + 4s^3}{3s^2} \tag{29}$$

The voltage transfer function takes the form

$$\frac{1}{2AB} = \left.\frac{0.5s^4}{14.222 + 98.667s + 253.56s^2 + 395.56s^3 + 402.39s^4 + 270.06s^5 + 113.33s^6 + 22.222s^7}\right|_{s = j\omega} \tag{30}$$

Data for the spectrum was found as before. The plot of the voltage transfer function versus angular frequency (see Fig. 19) shows that attenuation is higher than in the previous case for all frequencies. The phase angle dependence of this transfer function on angular frequency is presented in Fig. 20.

DEFINITION OF INTERACTANCE

In order to compare the power available at the input terminals of a filter with that which would be available if network were purely resistive, the concept "interactance" has been introduced by Fritzemeyer (1). Interactance is defined by

$$\Lambda = \frac{P_f}{P_r} \tag{31}$$

where Λ is the interactance of the filter; P_f is the power dissipated in the source resistance when the filter is connected, and P_r is the power dissipated in the source resistance when a

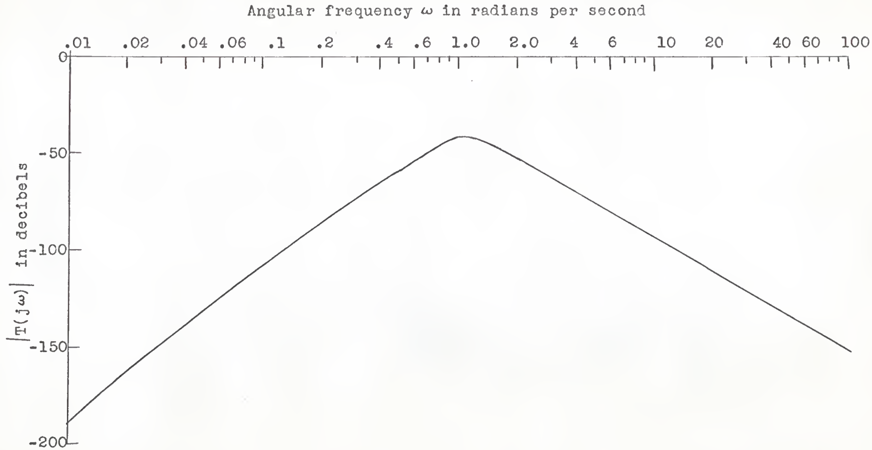

Fig. 19. Frequency response of no-pass filter of Fig. 18, where $\lambda = 0.5$

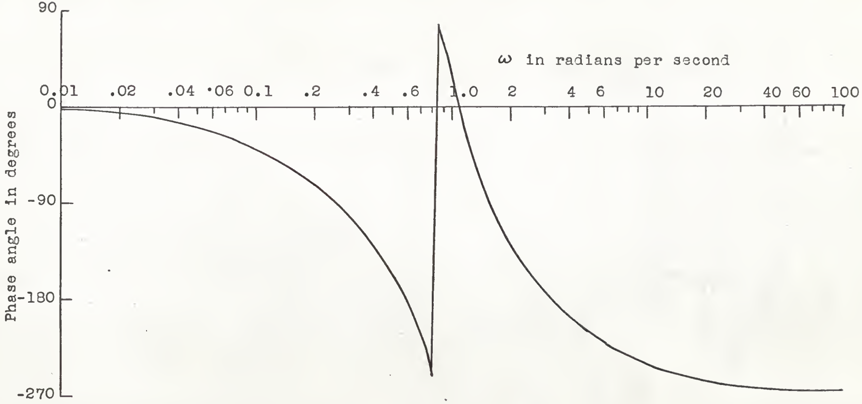

Fig. 20. Phase angle of voltage transfer function of no-pass filter of Fig. 18, where $\lambda = 0.5$

pure resistor equal to the source resistance replaces the filter in the circuit. In other words, the interactance of a filter is defined as the power dissipated in the source resistance to the power which would be dissipated if the maximum power were transferred to the filter. These powers, P_f and P_r, are measured with an additional voltage in the filter path (see Fig. 21), such that when the filter is replaced by a pure resistance the voltage across the source resistance is equal to the source voltage. Figure 22 shows the filter replaced by one ohm (which is pseudo-characteristic impedance of the filter) resistor.

Using Millman's theorem, the voltage e_{or} in Fig. 22 is

$$e_{or} = \frac{1(e) + 1(-e)}{1 + 1} = 0 \tag{32}$$

Therefore, the voltage across the source resistance is

$$e_r = e - e_{or} = e \tag{33}$$

where e is the source voltage. The power P_r, dissipated in the source resistance under these conditions is (assuming e is a peak value)

$$P_r = \frac{1}{2} \frac{|e|^2}{R} \tag{34}$$

If R is one ohm, the equation reduces to

$$P_r = \frac{1}{2} |e|^2 \tag{35}$$

Calculation of P_f follows a similar procedure except one ohm resistor is replaced by the input impedance of the filter as in figure 21.

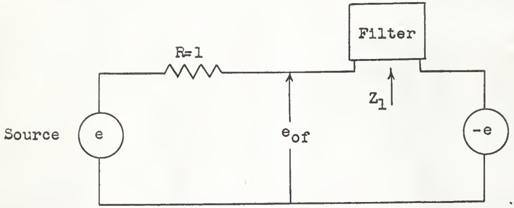

Fig. 21. Circuit for measurement of the interactance of a filter.

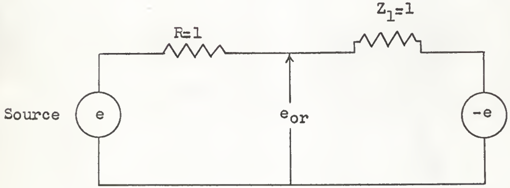

Fig. 22. Circuit for measurement of the interactance with filter replaced by one ohm resistor.

$$e_{of} = \frac{1(e) + \frac{1}{Z_1}(-e)}{1 + \frac{1}{Z_1}} \tag{36}$$

$$= \frac{Z_1(e) + (-e)}{Z_1 + 1} \tag{37}$$

The voltage across the source resistance for this case is

$$e_r = e - e_{of} \tag{38}$$

Substituting equation (37) into equation (38) yields

$$e_r = \frac{2(e)}{Z_1 + 1} \tag{39}$$

So the power P_f in this case is

$$P_f = \frac{1}{2}|e|^2 \left|\frac{2}{Z_1 + 1}\right|^2 \tag{40}$$

Substituting equations (35) and (40) in equation (31), the interactance of a filter is found to be

$$\Lambda = \left|\frac{2}{Z_1 + 1}\right|^2 \tag{41}$$

From equation (41), it is observed that interactance of a filter lies between zero and four for any input impedance of the filter and for all frequencies.

INTERACTANCE OF NO-PASS FILTER WITH $\omega_c' = \omega_c$

In order to find the interactance of the no-pass filter (see Fig. 14), input impedance Z_1 of the filter is first found. An extra series one ohm negative resistance is connected in the no-pass filter network of Fig. 14, as illustrated in Fig. 23. Input is related with output (see Fig. 23) by the expression

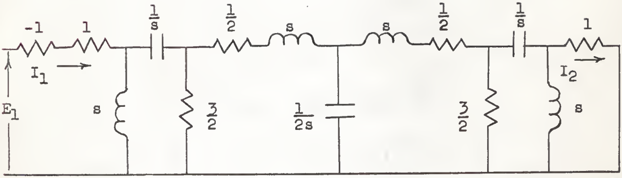

Fig. 23. Network of Fig. 14 with one ohm negative resistance attached on the input end for calculating the input impedance of the no-pass filter in Fig. 14.

$$\begin{bmatrix} E_1 \\ I_1 \end{bmatrix} = \begin{bmatrix} 1 & -1 \\ 0 & 1 \end{bmatrix} \begin{bmatrix} \beta\gamma + \alpha\delta & 2\alpha\beta \\ 2\delta\gamma & \beta\gamma + \alpha\delta \end{bmatrix} \begin{bmatrix} 0 \\ I_2 \end{bmatrix} \tag{42}$$

$$= \begin{bmatrix} 2\alpha\beta - (\beta\gamma + \alpha\delta) \\ \beta\gamma + \alpha\delta \end{bmatrix} (I_2) \tag{43}$$

Equation (43) can be written as

$$Z_1 = \frac{2\alpha\beta - (\beta\gamma + \alpha\delta)}{\beta\gamma + \alpha\delta} \tag{44}$$

$$= \frac{2\alpha\beta}{\beta\gamma + \alpha\delta} - 1 \tag{45}$$

$$Z_1 + 1 = \frac{2\alpha\beta}{\beta\gamma + \alpha\delta} \tag{46}$$

Substituting the value of $(Z_1 + 1)$ from equation (46), equation (41) yields

$$\Lambda = \left| \frac{\beta\gamma + \alpha\delta}{\alpha\beta} \right|^2 \tag{47}$$

Substituting the values of the parameters found in equations (19), (20), (21) and (22) in equation (47) yields

$$\Lambda = \left| \frac{1.7778 + 9.5556s + 21.222s^2 + 33.944s^3 + 35.056s^4 + 25.778s^5 + 12.444s^6 + 2.2222s^7}{0.88889 + 5.6667s + 15.389s^2 + 26.694s^3 + 30.556s^4 + 23.361s^5 + 11.667s^6 + 2.7778s^7} \right|^2_{s = j\omega} \tag{48}$$

By using an IBM 1620, data for the graph between interactance and angular frequency is obtained; the graph is plotted on log-log paper as shown in Fig. 24. It is noted that interactance is almost maximum and constant at very low frequencies,

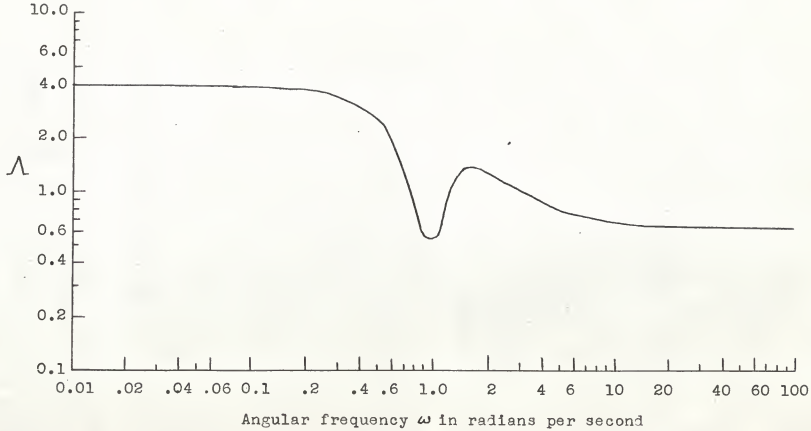

Fig. 24. Interactance of no-pass filter of Fig. 14.

but near cut-off frequency (one radian per second) of both related low-pass filter and high-pass filter there is a sudden variation. After the cut-off frequency it again becomes almost constant and has low value for all higher frequencies. This nonconformity to a single constant value indicates success for the characteristic impedance degradation program.

INTERACTANCE OF NO-PASS FILTER WITH $\omega_c' < \omega_c$

In this case when the cut-off frequency of the low-pass filter (see Fig. 18) is reduced to $1-\lambda$, i.e., 0.5 radian per second and the cut-off frequency of the high-pass filter is raised to $1/(1-\lambda)$ i.e., 2 radians per second, the new interactance function becomes (see Fig. 18)

$$\Lambda = \left| \frac{BC + AD}{AB} \right|^2 \tag{49}$$

Substituting the values of A, B, C and D from equations (26), (27), (28) and (29) respectively

$$\Lambda = \left| \frac{28.444 + 183.11s + 415.56s^2 + 586.88s^3 + 532.56s^4 + 318.22s^5 + 116.44s^6 + 17.778s^7}{14.222 + 98.667s + 253.56s^2 + 395.56s^3 + 402.39s^4 + 270.06s^5 + 113.33s^6 + 22.222s^7} \right|^2_{s = j\omega} \tag{50}$$

By using an IBM 1620, data for interactance plot is found, and the curve of Fig. 25 is obtained. It is noted that the transition near the cut-off is gradual and for other frequencies the interactance has desirable two constant behavior indicative of characteristic impedance degradation.

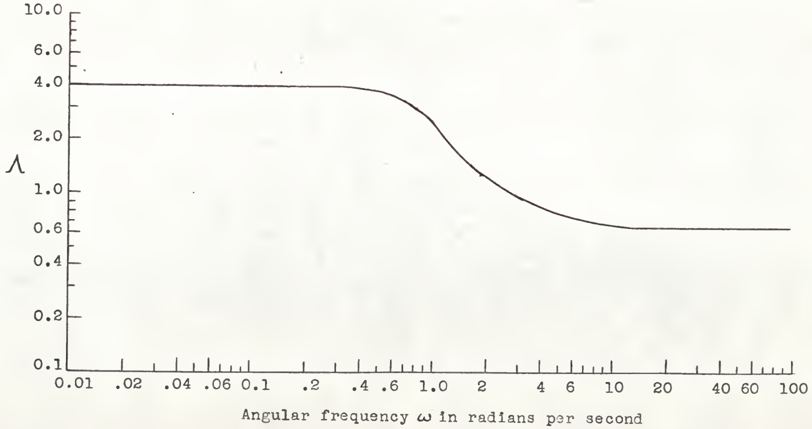

Fig. 25. Interactance of no-pass filter of Fig. 18, where $\lambda = 0.5$

SUMMARY

By definition a no-pass filter is obtained when a low-pass filter having the cut-off frequency ω_c' and a high-pass filter having the cut-off frequency ω_c are cascaded provided $\omega_c' \leqslant \omega_c$.

Previous work of Zobel on characteristic impedance improvement of a filter is reviewed in this report. He removed the shortcoming of constant-K filter design as regards characteristic impedance variation in the pass band.

Antithetical to Zobel's m-derivation method for characteristic impedance improvement, characteristic impedance degradation is accomplished by low- to high-pass transformation by emphasizing mismatching, and, as a consequence, the no-pass filter is realized. Frequency response of the transfer function of no-pass filter has been improved by lowering the cut-off frequency of its low-pass section, and correspondingly raising the cut-off frequency of the high-pass section. The plots of phase angle (in degrees) versus angular frequency (in radians per second) in both cases of transfer functions have also been presented.

The interactance of a filter is defined as the ratio of power dissipated in the source resistance with the filter in circuit to the power which would be dissipated if maximum power transfer conditions exist in the network. The plots of interactance of the no-pass filters versus angular frequency clearly show that the interactance does not conform to a single constant value indicating the desired characteristic impedance degradation.

ACKNOWLEDGMENT

The author wishes to express his deep appreciation to Dr. Charles A. Halijak of the Department of Electrical Engineering for his guidance and encouragement during the preparation of this report.

REFERENCES

1. Fritzemeyer, R. D.
   Fan-out Filters, A Master's Thesis, Kansas State University, 1963.

2. LePage, W. R., and Samuel Seely,
   General Network Analysis, New York: McGraw-Hill Book Company, Inc., 1952.

3. Lin, H. S.
   Annihilator Aspects of Transfer Functions, A Master's Report, Kansas State University, 1962.

4. Van Valkenburg, M. E.
   Network Analysis, Prentice-Hall, Inc., Englewood Cliffs, N.J., 1955.

5. Zobel, O. J.
   U. S. Patent 1,557,230.

APPENDIX

CAYLEY'S NOTATION

Cayley's notation for the bilinear transformation is demonstrated. Figures 26 and 27 show two four terminal networks. They are interconnected by cascade connection, as illustrated in Fig. 28. In Fig. 26 input-output relations are expressible in terms of network transfer coefficients a, b, c, d by the relations

$$E_1 = aE_2 + bI_2 \tag{51}$$

$$I_1 = cE_2 + dI_2 \tag{52}$$

The impedance looking into the network at the left is given by the ratio

$$Z_1 = \frac{E_1}{I_1} = \frac{aE_2 + bI_2}{cE_2 + dI_2} \tag{53}$$

The impedance $Z_2 = \dfrac{E_2}{I_2}$ (54)

Equation (53) can be written as

$$Z_1 = \frac{aZ_2 + b}{cZ_2 + d} \tag{55}$$

By Cayley's notation equation (56) can be written as

$$Z_1 = \begin{bmatrix} a & b \\ c & d \end{bmatrix} (Z_2)$$

Similarly in the other network in Fig. 27

Fig. 26. General four terminal network having a, b, c, d as its transfer coefficients.

Fig. 27. General four terminal network having a', b', c', d' as its transfer coefficients.

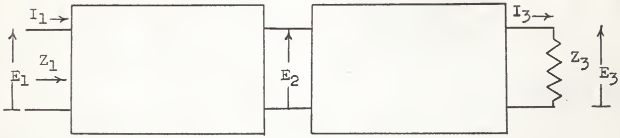

Fig. 28. Networks in figures 26 and 27 are connected in cascade.

$$Z_2 = \frac{a'Z_3 + b'}{c'Z_3 + d'} \tag{57}$$

and by Cayley's notation equation (57) can be written as

$$Z_2 = \begin{bmatrix} a' & b' \\ c' & d' \end{bmatrix} (Z_3) \tag{58}$$

Substituting equation (57) in equation (55) yields

$$Z_1 = \frac{a\dfrac{a'Z_3 + b'}{c'Z_3 + d'} + b}{c\dfrac{a'Z_3 + b'}{c'Z_3 + d'} + d} \tag{59}$$

$$= \frac{(aa' + bc')Z_3 + (ab' + bd')}{(a'c + c'd)Z_3 + (b'c + dd')} \tag{60}$$

By Cayley's notation equation (60) can be written as

$$Z_1 = \begin{bmatrix} (aa' + bc') & (ab' + bd') \\ (a'c + c'd) & (b'c + dd') \end{bmatrix} (Z_3) \tag{61}$$

In the cascaded network (see Fig. 28) equation (61) is also obtained as a matrix product if equation (58) is substituted in equation (56).

CLASSICAL NETWORK THEORY ASPECT OF NO-PASS FILTERS

by

TEJINDER SINGH RAJPAL

B. A., Panjab University, Chandigarh, India, 1958
B. Sc. Engg., Thapar Engineering College, 1962
Patiala, Panjab, India

AN ABSTRACT OF
A MASTER'S REPORT

submitted in partial fulfillment of the

requirements for the degree

MASTER OF SCIENCE

Department of Electrical Engineering

KANSAS STATE UNIVERSITY
Manhattan, Kansas

1964

In classical network theory filters are classified as low-pass filters, high-pass filters, band-pass filters, band-elimination filters and all-pass filters. When a low-pass filter and a high-pass filter are cascaded, the result is a band-pass filter provided cut-off frequency of the low-pass filter ω_c' is greater than that of the high-pass filter ω_c. But in case $\omega_c' \leqslant \omega_c$, the result is a no-pass filter.

Previous work of Zobel on characteristic impedance improvement of a filter has been reviewed. Antithetical to Zobel's m-derivation method for characteristic impedance improvement, characteristic impedance degradation is accomplished by low- to high-pass transformation by emphasizing mismatching, and, as a consequence, a no-pass filter is realized. Frequency response of the transfer function of the no-pass filter has been improved by lowering the cut-off frequency of the low-pass section, and correspondingly raising the cut-off frequency of the high-pass section. The phase angle dependence of the transfer functions on frequency has been presented.

The interactance of a filter is defined as the ratio of the power dissipated in the source resistance with the filter in circuit to the power which would be dissipated if the maximum power transfer conditions exist in the network. The plots of interactance of the no-pass filters versus angular frequency show that the interactance does not conform to a single constant value, which indicates the success for the characteristic impedance degradation program.